

HISTOLOGICAL AND IMMUNOHISTOCHEMICAL EVALUATION OF CHITOSAN–NANOHYDROXYAPATITE SCAFFOLD ON REGENERATIVE BONE HEALING IN OSTEOPOROTIC RABBITS

Hagar S. Gharib* , Hend M. Abdelhamid**  and Sara A. Hamza* 

ABSTRACT

Introduction: Chitosan is a biodegradable, naturally occurring polymer with recently used as a scaffold material in tissue engineering. To maximize the biocompatibility and bioactivity of Chitosan, nanohydroxyapatite has been incorporated into chitosan scaffolds.

Aim: This study aimed to investigate bone healing after placing CS/nHA scaffold in bone regeneration of extracted socket in rabbits with induced osteoporosis.

Materials and Methods: We used 40 New Zealand white rabbits randomly divided into 4 groups: group A (-ve Control), group B (+ve Control with CS/nHA scaffold), group C (osteoporosis with CS/nHA scaffold), and group D (osteoporosis without CS/nHA scaffold). After induction of osteoporosis and surgical extraction, the rabbits were euthanized at 2 and 6 weeks. The effect of CS/nHA was evaluated histologically and immunohistochemically using ALP, OP, and BMP-2 markers.

Results: Our results showed enhanced bone trabeculae in group B and C comparable with the group A. However, thin bone trabeculae with irregular bone surfaces were seen in group D. Our histological findings were confirmed by the newly formed bone surface area histomorphometry, besides ALP, BMP-2, and OP immunoexpression showing a sustained significant increase in group B and C compared with group D across both intervals.

Conclusion: The histology and immunoexpression of bone healing markers was positively affected by the placement of CS/nHA scaffolds under osteoporotic conditions. These results may indicate that CS/nHA scaffolds could be used to augment bone healing and improve the quality of newly formed bone after extraction in patients with osteoporosis required for future surgical procedures such as dental implantation.

KEYWORDS: Alkaline Phosphatase, Osteopontin, BMP2, Chitosan, Nanohydroxyapatite.

* Lecturer of Oral Biology Department, Faculty of Dentistry, Alexandria University, Egypt.

** Lecturer of Oral Pathology Department, Faculty of Dentistry, Alexandria University, Egypt.

INTRODUCTION

Bone reconstruction in the oral and maxillofacial regions allows esthetic and functional recovery of the craniofacial skeleton. The management of large bony defects caused by congenital anomalies, trauma, and degenerative disease remains a complicated problem for orthopedic reconstructive surgeons. To solve that, autologous bone grafts emerged as the gold standard for reconstructing bone defects. However, the main concern was the donor site morbidity and size limitations. This led to using bio-artificial bone tissues to overcome these drawbacks^[1]. Thus, bone tissue engineering is a distinctive new approach to bone regeneration^[2]. Within this field, biomedical polymers became a trendy material because of their biocompatibility and biodegradability. They are designed in the form of a three-dimensional (3D) scaffold with interconnected pores with high porosities. This facilitates the implantation of scaffolds in the human body. Hence, these scaffolds should have good biocompatibility, biodegradability, high porosity, and good mechanical properties^[3,4].

One of these biomedical materials is chitosan (CS), a popular natural polymer characterized by its biodegradability, biocompatibility, and nontoxicity^[5]. It can also be easily modified into different forms for orthopedic therapy, such as films, fibers, sponges, and complex forms. However, CS scaffolds exhibit poor mechanical properties because their flexibility makes them unsuitable for replacing normal bone. Meanwhile, CS scaffolds cannot support load-bearing bone implants^[6].

Chitosan scaffolds are mixed with hydroxyapatite (HA) to counter these limitations. This is the major inorganic bone component; given its high biocompatibility and osteoconductivity, it has been used as a suitable alternative for hard tissues. Moreover, it was used clinically as an artificial bone substitute for dental implants^[7]. This is performed mainly to overcome the high flexibility of CS.

However, the fragility and dispersion of hydroxyapatite (HA) granules make molding into the appropriate shape difficult; therefore, they are clinically restricted as bone substitutes^[8]. To solve this, HA is constructed in a nanoscale below 100nm in diameter. HA nanoparticles are characterized by their high bioactivity, biocompatibility, and flexibility, which are highly required in biomedicine. Since the nano-sized HA particles positively affect the host tissue response, the development of nanophase HA has been imperatively increasing^[9].

The combination of CS and nano HA (nHA) materials provide a composite with superior properties. It aids in improving cell adhesion and proliferation during new bone formation. Moreover, it increases mechanical strength, type I collagen production, and the expression of other osteogenic differentiation markers. CS/nHA scaffolds serve primarily as osteoconductive moieties, as new bone is deposited by creeping substitution from the adjacent living bone^[7,10,11].

Our study used a manufactured CS/nHA scaffold to induce bone healing in extracted sockets synthetically or obtained from natural sources^[12-14]. However, the composite of CS with synthetic HA is more widely used as a bone graft substitute instead of natural HA^[15].

Several bone disorders can jeopardize bone formation and subsequent mineralization. One of these diseases is osteoporosis. It is characterized by a reduction in bone density and structural deterioration, which increases the liability for silent fractures. Moreover, osteoporosis interferes with bone repair, even after a simple dental procedure such as exodontia^[14,16].

Osteoporosis treatment is divided into antiresorptive (anti-catabolic), anabolic, and combination. Osteoclasts remain the main targets of medical intervention. Moreover, it is crucial to reverse bone loss and stimulate bone formation by boosting bone regeneration, which has become a challenge

for health care providers ^[17]. Osteoanabolic therapy such as bisphosphonates, denosumab, and estrogen activates bone formation because of its effects on osteoblasts, and the only currently available treatment regimen is the daily injection of one of the analogs of parathyroid hormone (PTH). However, a higher risk of adverse effects, mainly cardiovascular symptoms, is associated with systemic administration ^[18]. Thus, for dental manipulation, a locally applied material with a bone regenerative capacity to induce adequate bone density in patients with osteoporosis is highly encouraged ^[16].

Within this context, we were interested in investigating a panel of bone markers upregulated during bone healing after placement of our designed CS/nHA scaffold that induced bone formation. Bone morphogenetic protein 2 (BMP-2) is a key player factor in osteogenesis, which induces the differentiation of mesenchymal stem cells into osteoblasts. Moreover, alkaline phosphatase (ALP) is a key player and a widely used osteoblast biomarker responsible for regulating osteoblast function and extracellular matrix mineralization during bone remodeling ^[19]. Finally, we used osteopontin (OP) to investigate the early stages of bone mineralization, as it is located along the wounded surface, allowing osteoblasts to integrate and promote bone mineralization through cement line bonding ^[20].

This study aimed to evaluate immunohistochemical markers of bone healing profiles such as ALP, BMP-2, and OP after placing the CS/nHA scaffold in induced osteoporotic rabbits.

MATERIAL AND METHODS

Experimental animals

The study was conducted in accordance with the ethical guidelines of research on experimental animals at the Faculty of Dentistry, Alexandria University (IRB No. 00010556-IORG 0008839). Forty 6-month-old (3.5–4.5 kg weight) white New Zea-

land rabbits were used in this study. Animals were obtained from the animal house of the Medical Research Institute, Alexandria University. They were housed in the experimental animal house under the same nutritional and environmental conditions ^[21]. Rabbits involved in an earlier experimental study or suffering from diseases or injuries were excluded.

Rabbits were divided randomly by computer-assisted software into four equal groups: group A (- ve control), group B (+ ve control with CS/nHA scaffold), group C (osteoporosis with CS/nHA scaffold, study group), and group D (osteoporosis without CS/nHA scaffold). A random allocation was completed using a computer-generated random sequence of numbers to assign treatment status to reduce the possibility of error, in which all personnel who performed the tests were unaware of the treatment assignment ^[22].

Characterization of the scaffold and the nanohydroxyapatite particles

For this study, we used a prefabricated CS/nHA scaffold designed and provided by a nanotechnology company (Nano Tech Egypt, 6th of October City, Egypt). The morphology and size of the scaffold's pores were characterized using scanning electron microscopy (SEM, JSM-5300, JEOL, Japan) to show interconnected pores and verify nHA incorporation in the CS scaffold. The characterization was completed at the Faculty of Science, Alexandria University, Egypt. The scaffold was cut by a razor blade, mounted on aluminum stubs with conductive paint, and then sputter-coated with gold for examination ^[23,24]. Moreover, we verified the size and shape of the nHA using a transmission electron microscope (TEM, JOEL, 1400plus, Japan) at the Faculty of Science, Alexandria University, Egypt.

Induction of osteoporosis

Osteoporosis was induced using weight-related dose adaptations of sodium succinate methylprednisolone (EPICIO, Nasr City, Egypt).

Osteoporosis was performed only for groups C and D. Rabbits were injected with 2 mg/kg/day of sodium succinate methylprednisolone intramuscularly over four consecutive weeks. By the end of week 4 post-injection, the rabbits were prepared for surgical extraction of the mandibular right first premolar [16].

Surgical procedure and CS/nHA scaffold application

After 4 weeks of osteoporosis induction, the animals were sedated using a combination of 13 mg/kg xylazine hydrochloride and 33 mg/kg ketamine and prepared for atraumatic extraction of the right mandibular first premolar [25]. After that, for rabbits in group D, the extraction sockets were left for spontaneous healing without using any material. However, the sockets in groups B and C were packed with CS/nHA scaffolds. Then, 4-0 Vicryl sutures were used to close the soft tissue of all groups using a cross-mattress technique to achieve site stability.

After the surgery, five animals from each group were euthanized after 2 and 6 weeks. The mandibles were dissected, and the right halves were separated and prepared for histological and immunohistochemical examinations. Finally, any animal disposals were burned.

Histological evaluation of bone regeneration

After sacrifice, extracted biopsies were immediately placed in 10% formalin and subsequently immersed into 0.5 M ethylene diamine tetra acetic acid tamponade for (10–15 days) for demineralization. They were dehydrated using 95% ethanol for 6 h after rinsing with water. Thus, the biopsies were soaked for 5 h in xylene, 5 h in paraffin, and eventually integrated into liquid paraffin. With microtome, sections of 4 μ m thickness were cut [26]. Each section was stained with hematoxylin/eosin (H&E) and examined under a light microscope for further investigations.

Histomorphometric analysis

The histologic tissue sections were quantitatively analyzed using ImageJ 1.46 r software (all obtained a magnification of $\times 100$) to calculate the mean percentage (%) of the newly formed bone surface area [27]. Five images were analyzed for each tissue section by two pathologists blindly for the four groups at two-time intervals.

Immunohistochemical evaluation

The prepared tissue sections were stained using ALP (at a dilution ratio of 1:50 of rabbit polyclonal anti-ALP antibody), BMP-2 (at a dilution ratio of 1:50 of mouse polyclonal anti-BMP-2 antibody), and OP (at a dilution ratio of 1:50 of rabbit polyclonal anti-OP antibody). Immunohistochemical staining was achieved by the labeled streptavidin-biotin method [28]. Evaluation was performed by two investigators in randomly selected microscopic fields at a magnification of 400 \times to determine the intensity of the three immune stains as the mean area percentage. Data were analyzed quantitatively using ImageJ 1.46 r. Moreover, positive cells were counted in five microscopic fields that demonstrated more intense staining.

Statistical analysis

Data were analyzed using GraphPad Prism (version 8, GraphPad Software Inc., LCC). Normality was checked for all variables using descriptive statistics, plots (histogram and boxplots), and the Shapiro-Wilk normality test. All variables showed normal distribution; thus, means and standard deviation (SD) were calculated, and parametric tests were used. The distributions of quantitative variables were tested using the F-test (analysis of variance). The level of significance ($p < 0.05$) was indicated on plots with asterisks (*). A sample of 40 rabbits is needed to detect a reduced significant difference in bone regeneration among the groups treated with CS/nHA compared with the osteoporotic group. The sample size was estimated assuming an 80% study power and 5% alpha error. Following Chatzipet-

ros et al. [15], the mean (SD) surface area of newly formed bone was 91733.0 (38855.6) when the CS/nHA scaffold was used and 46762.17 (25507.97) when no scaffold was used. Based on the comparison of means, the calculated sample size was 9 per group, which was increased to 10 to make up for laboratory processing errors. The total required sample size was as follows: the number of groups \times number per group = $4 \times 10 = 40$.

RESULTS

Using the osteoporotic rabbit model treated by the CS/nHA scaffold, we noticed a generalized improvement in bone quality at 2 and 6 weeks post-extraction. Group B and C, treated with CS/nHA, had regular and rapid woven bone formation with many osteocytes inside its lacunae, indicating an active bone formation compared with group D at 2 weeks. Furthermore, 6 weeks after extraction, groups B and C sockets were comparable and showed more regular and mature bone formation with many osteocytes inside its lacunae compared with those of group D.

Characterization of the CS/nHA scaffold and nHA particles

Scanning electron microscopy analysis of the CS/nHA scaffold revealed almost spherical,

interconnected, regular pores, with sizes ranging from 20 to 400 μm and dense struts in between (Fig. 1a). The nHA particles were homogeneously embedded like islands within a high density on the surface of the scaffold and scattered in the pore wall surfaces of the scaffold (Fig. 1b). Moreover, TEM examination showed that nHA particles are mostly rod or needle-like in shape with uniform size ($<100\text{nm}$ in length and 20–25 nm in diameter) (Fig. 1c).

Histologic evaluation

We examined the tissue sections extracted from the rabbits to identify the successive regenerative changes in osteogenesis following the application of the CS/nHA scaffold in osteoporotic rabbits.

At 2 weeks (Fig. 2 a-d), the healing socket in the control group was filled with fibrous tissue and thin bone spicules lined by active osteoblasts and large osteocytes, while group B showed the healing socket filled with thin spicules of newly formed bone, which were lined by voluminous osteoblasts and contained numerous osteocytes with relatively wide lacunae. Meanwhile, group C osteoporosis that received CS/nHA scaffold demonstrated regenerative features, where the amount of newly formed bone was comparable with what was noted

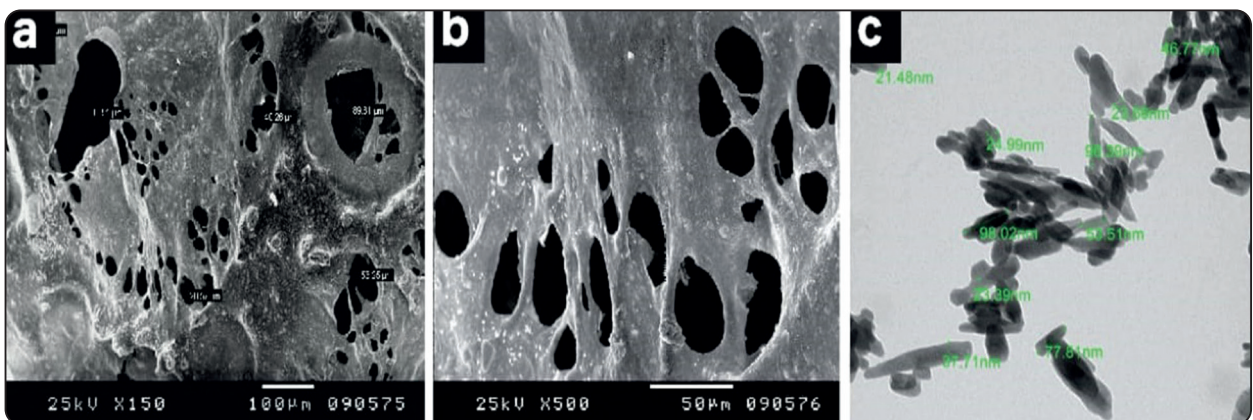


Fig. 1: a Scanning electron micrograph of the CS/nHA scaffold showing spherical, interconnected pores, and dense struts ($\times 150$). b Showing higher magnification of nHA particles attached to the surface of the scaffold (red circle) ($\times 1500$). c Transmission electron micrograph of nanohydroxyapatite (nHA) suspension showing that most of the nanoparticles are rod or needle-like with average particle size ranging from 20 to 50 nm ($\times 2000$).

in group A. Moreover, the sockets exhibited a more significant amount of immature woven bone near the scaffold. Numerous active osteoblasts with plump nuclei lined the bone surface with osteocytes. However, group D presented with very thin newly formed bone trabeculae, with irregular outlines, consisting of numerous osteoclasts with Howship's lacunae giving a punched-out appearance compared with those in group C. We noticed a discontinuity of the osteoblasts along the alveolar bone border.

At 6 weeks (Fig. 2 e–h), in group A, showing normal bone healing at this interval with normal bone trabeculae lined by few active osteoblasts and some regular osteocytes surrounding normal bone marrow spaces. In addition to resting and reversal lines. While group B, bone maturation continues with the presence of active plump osteoblasts lining the thick bone trabeculae surface and bone marrow

spaces. In addition, osteocytes were regularly distributed in its lacunae with rounded nuclei. Finally, several resting and reversal lines could be obviously noted. For group C, the bone trabeculae were thick and regularly distributed with areas of smooth surfaces and surrounded by bone marrow spaces with scaffold fragments. Furthermore, several resting and reversal lines could be obviously seen. An outstanding fashion of active voluminous osteoblast cells lined the bone surface. Moreover, osteocytes were with their prominent nuclei entrapped within a relatively wide lacuna. On the contrary, rabbits in group D showed an irregular bone surface with punched-out margins. Few osteoblasts were found lining the bone surface with fewer haphazardly arranged osteocytes with relatively narrow lacunae when compared with those in group C. Additionally, several scalloping remodeling lines could be observed.

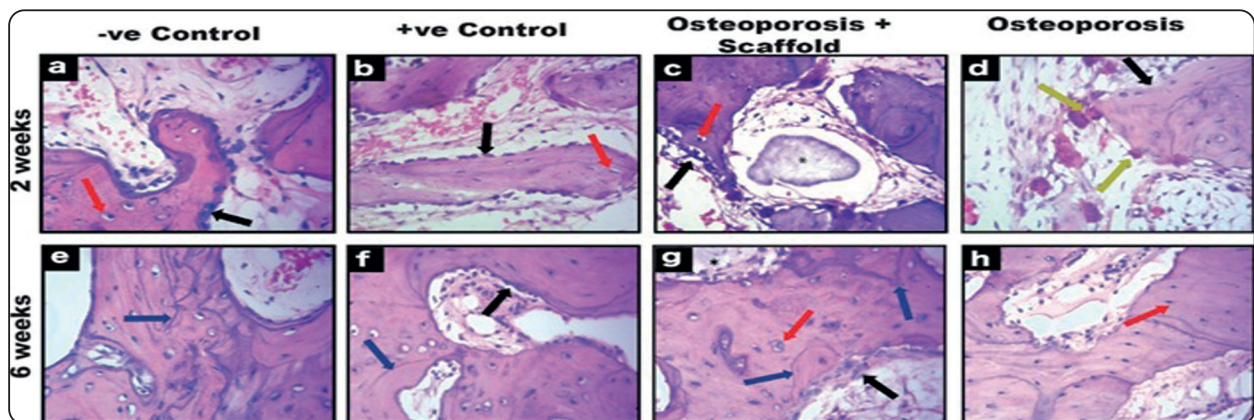


Fig. (2) Histologic evaluation of the CS/nHA scaffold at 2 and 6 weeks. a Group A (-ve Control) at 2 weeks, revealing: Healing socket filled with fibrous tissue and thin bone spicules lined by active osteoblasts and osteocytes in large lacunae. b Group B (+ve Control with CS/nHA scaffold) at 2 weeks, illustrating: Active osteoblast lining the bone trabeculae surface and bone marrow spaces, in addition to regularly distributed osteocytes in its lacunae with rounded nuclei were seen. c Group C (osteoporosis with CS/nHA scaffold) at 2 weeks showing remnants of the scaffold (denoted by an asterisk) close to the newly formed bone with voluminous osteoblasts lining and regular osteocytes. d Group D (osteoporosis without CS/nHA scaffold) at 2 weeks exhibiting numerous prominent osteoclasts inside Howship's lacunae with irregular bone trabeculae with discontinuity of osteoblasts on its surface are seen. e At 6 weeks, Group A (-ve control) showing: Normal bone trabeculae lined by few active osteoblasts and some regularly arranged osteocytes. Note regular resting and reversal lines. f At 6 weeks, Group B (+ve Control with CS/nHA scaffold) shows thick trabecular bone lined by osteoblasts and accentuated reversal lines. g Group C (osteoporosis with CS/nHA scaffold) at 6 weeks showing bone trabeculae covered by active, plump crowded osteoblasts with prominent, large nuclei in osteocytes with numerous reversal lines. The bone marrow space was filled with dissociated fragments of the scaffold (asterisk). h Group D (osteoporosis without CS/nHA scaffold) at 6 weeks demonstrated irregular, thin punched-out bone surface with several remodeling lines and few osteocytes (black arrow, osteoblasts; red arrow, osteocytes; yellow arrow, osteoclasts; and blue arrow, reversal line) (All images are stained with H&E stain; $\times 400$).

Histomorphometric analysis

After histologic examination of the bone healing histologically, we quantified the newly formed bone surface area in the healing sockets for the four groups after 2 and 6 weeks. For both time intervals, we noted a significant increase in the percentage of the newly formed bone surface area in groups A, B and C compared with group D; as well there is no significant difference between groups A and B. There is a significant increase in bone surface area between groups B and C at 2 weeks; However, there is no significance difference between both groups at 6 weeks (week 2: group A, 7.5 ± 1.5 ; group B, 8.4 ± 0.9 ; group C, 6.2 ± 1 ; group D, 3.5 ± 1.1 ; $P < 0.005$) (week 6: group A, 12 ± 1.9 ; group B, 12.9 ± 2.4 ; group C, 12 ± 2.2 ; group D, 7.6 ± 1.3 ; $P < 0.005$) (Fig. 3)

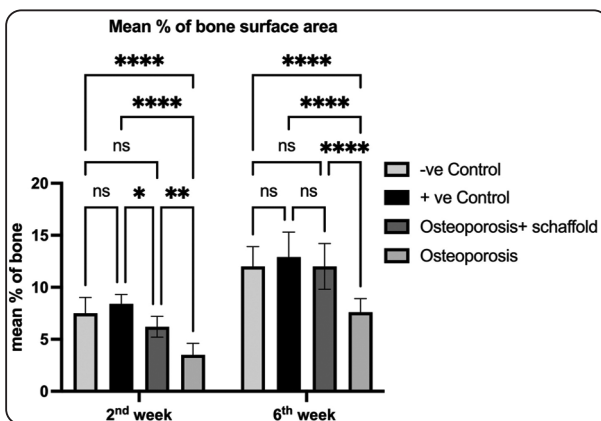


Fig. (3) A representative graph showing the difference in the mean percentage of the bone surface area in all groups. A significant increase in the mean percentage of the bone surface area in groups B and C compared with group D was seen at all study periods (2 and 6 weeks), with a significant difference between groups Band C at 2 weeks; However there is no significant difference between them at 6 weeks ($P < 0.05$; denoted by asterisks).

Immunohistochemical analysis

We examined the extracted tissue specimens across groups A, B, C and D using ALP, BMP-2, and OP immunostaining at 2 and 6 weeks. At 2 weeks, a significant difference in BMP-2 and OP immunoreaction was found among the groups (BMP-2: group A, 61.80 ± 3.80 ; group B, 65.87 ± 6.41 ; group C, 58.40 ± 4.52 ; group D, 27.91 ± 9.20 ; OP, group A 62.40 ± 4.20 ; group B, 66.32 ± 4.83 ; group C, 56.89 ± 5.79 ; group D, 29.22 ± 3.34 ; $P < 0.0001^*$). However, the increase in ALP immunoexpression between group B and group C was not significant (ALP: group A, 60.21 ± 4.50 ; group B, 63.55 ± 6.7 ; group C, 55.14 ± 6.08 ; $P = 0.219107$). Significant ALP immunostaining was noted between groups B and C compared to group D (ALP: group B, 63.55 ± 6.7 ; group C, 55.14 ± 6.08 ; group D, 28.60 ± 8.28 ; $P < 0.001^*$) (Fig. 4 a–m).

At 6 weeks, a generalized decline in all immunohistochemical reactions of ALP, BMP-2, and OP was seen among the four groups upon bone maturation. For ALP, BMP-2 and OP a significant decrease in the immunoreaction was noted during this time interval among the four groups (ALP: group A, 40.76 ± 3.40 ; group B, 44.27 ± 4.09 ; group C, 50.96 ± 6.02 ; group D, 13.97 ± 4.48 ; BMP-2: group A, 28.54 ± 5.10 ; group B, 33.92 ± 4.02 ; group C, 36.81 ± 2.56 ; group D, 18.54 ± 3.71 ; OP: group A, 27.59 ± 2.80 ; group B, 33.78 ± 2.54 ; group C, 30.81 ± 2.54 ; group D, 18.67 ± 3.65 ; $P < 0.0001^*$). No significant difference was noted between groups A and B for the 3 immunohistochemical markers. On the contrary, a significant decrease for all immunostaining was noted in group D compared with groups A, B and C (Fig. 5 a–m).

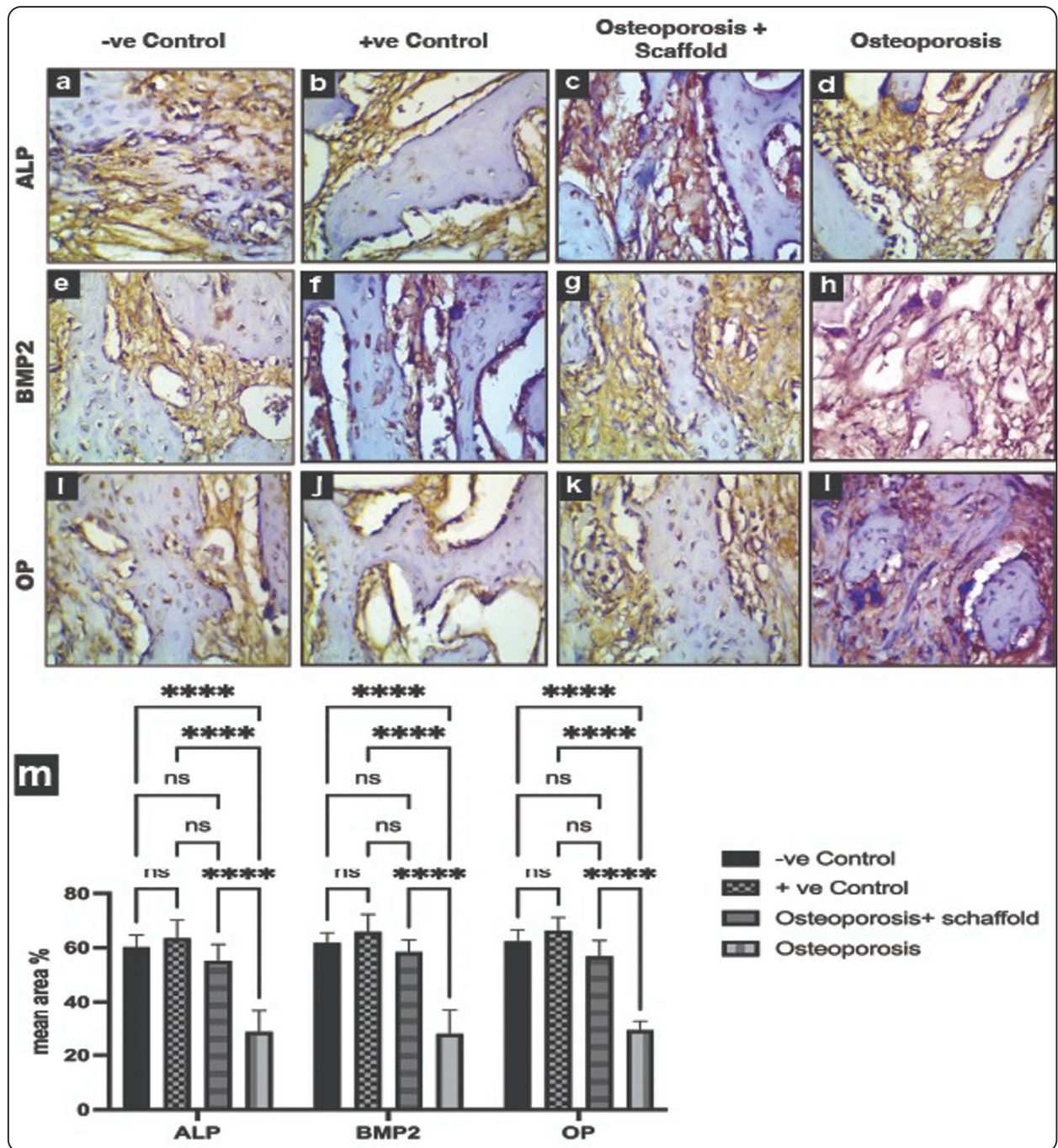


Fig. (4) Immunohistochemical profile of ALP, BMP-2, and OP in 2 weeks. a-d Photomicrographs showing changes in ALP immunostaining between the three different groups. e-h Photomicrographs showing the difference in BMP-2 immunostaining among the three groups. i-l Photomicrographs revealing variation in OP immunosignals among the three groups. m A representative graph illustrating the 2-week mean area percent for ALP, BMP-2, and OP immunostaining among groups A, B, C and D showing a significant difference between ALP, BMP-2, and OP among the four groups, however the difference between groups A, B and C was not significant ($P < 0.001$ * denote by asterisks. All sections are at $\times 400$ magnification).

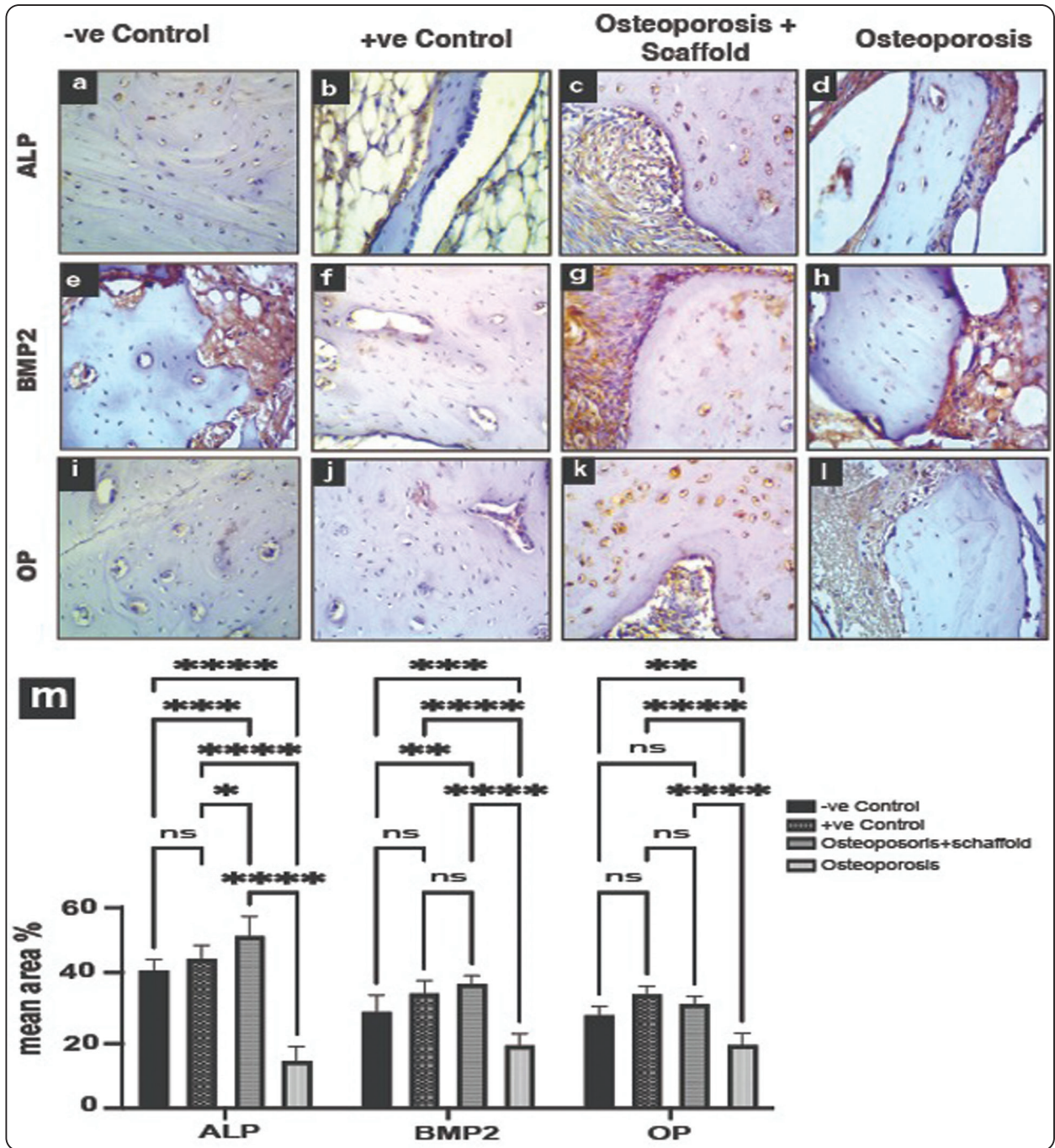


Fig. (5) Immunohistochemical profile of ALP, BMP-2, and OP in 6 weeks. a-d Photomicrographs showing changes in ALP immunostaining between the four different groups. e-h Photomicrographs showing the difference in BMP-2 immunorexpression among the four groups. i-l Photomicrographs revealing variation in OP immunosignals among the four groups. m A representative graph illustrating the 6-week mean area percent for ALP, BMP-2, and OP immunostaining between groups A, B, C and D showing a significant difference between ALP, BMP-2, and OP among group D and the other three groups. A sustained significant decrease in ALP, BMP-2, and OP immunorexpressions in group D was noted compared with those in groups A, B and C. ($P < 0.001^*$; denoted by asterisks). All sections are at $\times 400$ magnification.

DISCUSSION

Healing an extracted socket requires bone regeneration, consisting of a well-organized sequence of biomonitoring events. It involves the interaction of bone cells controlled by intracellular or extracellular signaling pathways. Several investigations have been conducted to speed up this process with superior bone quality^[29,30]. On the contrary, bone regeneration is highly influenced by some metabolic disorders that affect bone mineralization, such as osteoporosis. Furthermore, several trials have been conducted to develop newly designed materials for bone regeneration that possess the ability to stimulate the newly forming bone tissues and repair bone defects^[31]. nHA is one of these materials that belong to ceramic-based bone graft alternatives owing to its biocompatibility, and it is considered one of the main constituents of bone tissues. Moreover, nHA can mimic the dimensions of constituent components of calcified tissues such as bone and teeth^[32]. Within that context, we used CS/nHA composite scaffolds in the extraction sockets of osteoporotic rabbits and evaluated the scaffold effect after 2 and 6 weeks.

Hence, H&E staining was performed, followed by an examination of the tissue sections at two follow-up intervals, i.e., 2 and 6 weeks postoperatively. This was conducted to show the status of bone-forming cells and the distinction between immature woven bone and mature lamellar bone^[26].

Our histologic results showed that the socket of osteoporotic rabbits treated with CS/nHA has more regular and rapid woven bone formation with numerous active osteoblasts with osteocytes inside its lacunae, similar to groups A and B. On the contrary, the socket of group D had an uneven, resorptive (pitted) surface, and very thin bony spicules were identified at the surface of a freshly created bone. In this study, we used CS/nHA scaffold with a high concentration and uniform distribution of nHA granules in the CS matrix, which contributed to the high bioactivity and sufficient mechanical

strength of the scaffolding material^[33]. Moreover, to enhance the bioactivity of the material, it is better to mimic the hybrid composition of the natural bone and enhance the mechanical strength of the scaffold. The 3D pore structures of our CS/nHA scaffold facilitate cell adhesion, differentiation, and proliferation, which aid in early osteoinduction^[33]. Meanwhile, the microporosity (pores < 20 mm) of our CS/nHA scaffold enhances the surface area for protein adsorption and offers attachment sites for osteoblasts to promote bone formation into scaffolds^[34]. This may indicate the osteoinductive capabilities of our CS/nHA scaffold under a light microscope for osteoporotic rabbits in 2 weeks.

At 6 weeks, the newly formed bone in the sockets of both groups B and C continues its maturation. We noted active osteoblasts lining the bone trabeculae surface and bone marrow spaces with several resting and reversal lines compared with the thin and punched-out surface of the bone trabeculae in the osteoporotic group. Moreover, several small remnants of the CS/nHA scaffold were seen in group C enclosed within the newly formed bone trabeculae, which indicate the slow biodegradation of the CS/nHA scaffold, as it may persist until 16 weeks postoperatively^[14]. This slow biodegradation may be the reason for the activation of the voluminous osteoblasts arranged on the bone surface, as seen by Lee et al.^[14]. This could be related to the contents of CS and the diameter of nHA powder used on our scaffold. This could be explained by the capability of chitosan to promote the cell adhesion and proliferation of osteoblast-related cells, as well as it can act as an ideal carrier for bone-promoting substances. This is owing to its natural polysaccharide structure that is similar to glycosaminoglycan sulfate (one of the main components of collagen fibers in the extracellular matrix (ECM)). This allows CS to provide a microenvironment for cell proliferation and ECM, and has the potential to promote bone formation. The positive charge on CS amino group, allows it to bind to the cell membrane, thereby providing the appropriate conditions for cell adhesion^[35].

We were further interested in studying the ALP, BMP-2, and OP immune profiles to assess the effect of the CS/nHA scaffold on the molecular level to support our histologic findings. During the first interval, our CS/nHA scaffold increased the level of ALP immunostaining in group C comparable with that of the control groups A and B. Meanwhile, group D extraction sockets revealed significantly lower ALP, as seen also by Zhao et al. in their study [36]. This is often related to significant osteoblast adhesion with the cell's filopodia adhering to the nHA and aiding in higher differentiation levels of osteoblasts [37]. Moreover, when we assessed BMP-2 immune reaction, BMP-2 immunostaining was significantly higher in the CS/nHA scaffold osteoporotic group C than in group D. Thus, the CS/nHA scaffold may be the reason for the high BMP-2 immune reaction, as it mediates the signaling cascade for the BMP-2 pathway after 2 weeks [38]. Furthermore, Lai et al. indicated that integrins interplay with BMP-2 receptors and play an essential role in BMP-2 induction of osteoblast differentiation from mesenchymal osteoprogenitor cells [39].

During the second interval after 6 weeks postoperatively, there was a depression in the expressions of the three bone markers ALP, BMP-2, and OP. This was explained by the presence of ALP, BMP-2, and OP served as an early differentiation marker and effective marker of bone formation, which was in line with the results of Oliveira et al. [40]. They showed that there is a depression in the level of bone markers in later stages of bone healing as the bone is in the maturation stages [40]. In addition, the slow degradation rate of the CS/nHA scaffold may help in maintaining the presence of bone markers. The immune reactivity against OP in group C showed similar results to the control groups A and B; however, the osteoporotic group D was less than the control groups A and B. OP is a component of the mineralized extracellular matrix crucial for biomineralization in bone remodeling. In addition to osteoprogenitor proliferation, matrix maturation and cell mineralization are two final stages in osteoblast development [41]. On the other hand, there was a significant decrease in bone markers in

group D than the other three groups. This was in accordance with Raje et al who suggested reduced transcriptional activity of BMP-2 promoter as well as decreased gene expression in an osteoporotic condition [42].

Based on the results of our histological results and the analysis of bone regeneration immunohistochemical markers, the CS/nHA scaffold can enhance bone regeneration in cases of osteoporosis to a level similar to normal conditions. However, the CS/nHA scaffold requires *in vivo* validation before it can be used for bone tissue engineering.

Nevertheless, this study has some limitations, as it needs to increase the study duration (8 and 12 weeks) to examine the rate of nHA absorption; thus, further research is recommended to be conducted for that reason. In addition, future research is suggested to be done to assess the effect of the CS/nHA scaffold on the stem cells to obtain a detailed description of its effect on bone healing.

CONCLUSION

We found that CS/nHA scaffolds can act as osteoconductive material aiding in bone regeneration. Moreover, upon application, it might be used to counteract the effect of osteoporosis. Therefore, it might be helpful for future surgical procedures during dental implantation in patients with osteoporosis.

Competing interests

The authors declare they have no conflict of interest.

Funding

No funding is subjected to the research reported in this manuscript.

Ethics approval

The study was conducted following the ethical guidelines for the conduct of research on experimental animals by the Faculty of Dentistry, Alexandria University (IRB No. 00010556-IORG 0008839).

Informed consent

Not applicable.

Availability of data and materials

All data included in this study are available from the corresponding author upon request.

Authors' contributions

HS, HA, and SH equally contributed to the conceptualization, methodology, validation, data curation, investigation, resources, writing-original draft preparation, visualization, and writing-reviewing and editing of the paper.

RECOMMENDATIONS

According to the results of the present study, we recommend the following:

1. More studies are needed to detect the effect CS/nHA scaffold on bone healing at different intervals
2. Further investigations should be administered to evaluate other bone healing markers.
3. More studies are required to study the effect CS/nHA scaffold on healing of critical size alveolar bone defects.

REFERENCES

1. Marcacci M, Kon E, Moukhachev V, Lavroukov A, Kutepov S, Quarto R, Mastrogiacomo M, Cancedda R. Stem cells associated with macroporous bioceramics for long bone repair: 6- to 7-year outcome of a pilot clinical study. *Tissue Eng.* 2007;13:947-55.
2. Miranda SC, Silva GA, Hell RC, Martins MD, Alves JB, Goes AM. Three-dimensional culture of rat BMMSCs in a porous chitosan-gelatin scaffold: A promising association for bone tissue engineering in oral reconstruction. *Arch Oral Biol.* 2011;56:1-15.
3. Price RL, Waid MC, Haberstroh KM, Webster TJ. Selective bone cell adhesion on formulations containing carbon nanofibers. *Biomaterials.* 2003;24:1877-87.
4. Yang S, Leong KF, Du Z, Chua CK. The design of scaffolds for use in tissue engineering. Part I. Traditional factors. *Tissue Eng.* 2001;7:679-89.
5. VandeVord PJ, Matthew HW, DeSilva SP, Mayton L, Wu B, Wooley PH. Evaluation of the biocompatibility of a chitosan scaffold in mice. *J Biomed Mater Res.* 2002;59:585-90.
6. Pallela R, Venkatesan J, Janapala VR, Kim SK. Biophysical-chemical evaluation of chitosan-hydroxyapatite-marine sponge collagen composite for bone tissue engineering. *J Biomed Mater Res A.* 2012;100:486-95.
7. Konishi S, Nakamura H, Seki M, Nagayama R, Yamano Y. Hydroxyapatite granule graft combined with recombinant human bone morphogenetic protein-2 for solid lumbar fusion. *J Spinal Disord Tech.* 2002;15:237-44.
8. Chen F, Wang ZC, Lin CJ. Preparation and characterization of nano-sized hydroxyapatite particles and hydroxyapatite/chitosan nano-composite for use in biomedical materials. *Mater Lett.* 2002;57:858-61.
9. Chen F, Lam WM, Lin CJ, Qiu GX, Wu ZH, Luk KD, et al. Biocompatibility of electrophoretical deposition of nanostructured hydroxyapatite coating on roughen titanium surface: in vitro evaluation using mesenchymal stem cells. *J Biomed Mater Res B Appl Biomater.* 2007;82:183-91.
10. Groeneveld EH, van den Bergh JP, Holzmann P, ten Bruggenkate CM, Tuinzing DB, Burger EH. Mineralization processes in demineralized bone matrix grafts in human maxillary sinus floor elevations. *J Biomed Mater Res.* 1999;48:393-402.
11. Huang Z, Feng Q, Yu B, Li S. Biomimetic properties of an injectable chitosan/nano-hydroxyapatite/collagen composite. *Mater Sci Eng C.* 2011;31:683-7.
12. Bezzi G, Celotti G, Landi E, La Torretta TM, Sopyan I, Tampieri A. A novel sol-gel technique for hydroxyapatite preparation. *Mater Chem Phys.* 2003;78:816-24.
13. Koutsopoulos S. Synthesis and characterization of hydroxyapatite crystals: a review study on the analytical methods. *J Biomed Mater Res.* 2002;62:600-12.
14. Lee JS, Baek SD, Venkatesan J, Bhatnagar I, Chang HK, Kim HT, et al. In vivo study of chitosan-natural nano hydroxyapatite scaffolds for bone tissue regeneration. *Int J Biol Macromol.* 2014;67:360-6.
15. Chatzipetros E, Christopoulos P, Donta C, Tosios KI, Tsiambas E, Tsiourvas D, et al. Application of nano-hydroxyapatite/chitosan scaffolds on rat calvarial critical-sized defects: A pilot study. *Med Oral Patol Oral Cir Bucal.* 2018;23:e625-e32.

16. Lin T, Liu J, Yang S, Liu X, Feng X, Fu D. Relation between the development of osteoporosis and osteonecrosis following glucocorticoid in a rabbit model. *Indian J Orthop.* 2016;50:406-13.
17. Tabacco G, Bilezikian JP. Osteoanabolic and dual action drugs. *Br J Clin Pharmacol.* 2019;85:1084-94.
18. Föger-Samwald U, Dovjak P, Azizi-Semrad U, Kersch-Schindl K, Pietschmann P. Osteoporosis: Pathophysiology and therapeutic options. *EXCLI J.* 2020;19:1017-37.
19. Sun J, Li J, Li C, Yu Y. Role of bone morphogenetic protein-2 in osteogenic differentiation of mesenchymal stem cells. *Mol Med Rep.* 2015;12:4230-7.
20. Anwar SK, Hamid HMA. Immuno-histopathologic evaluation of mineralized plasmatic matrix in the management of horizontal ridge defects in a canine model (a split-mouth comparative study). *Odontology.* 2022;110:523-34.
21. Navia JM. University of Alabama Press. Animal models in dental research. *Int J Oral Maxillofac Surg.* 1977;17:82-3.
22. Muhlhauser BS, Bloomfield FH, Gillman MW. Whole animal experiments should be more like human randomized controlled trials. *PLoS Biol.* 2013;11:e1001481.
23. O'Brien FJ. Biomaterials & scaffolds for tissue engineering. *Mater Today.* 2011;14:88-95.
24. Hosokawa M, Nogi K, Naito M, Yokoyama T. Nanoparticle technology handbook. 2nd ed. Amsterdam: Elsevier; 2012. 5-51.
25. Kotsakis G, Chrepa V, Marcou N, Prasad H, Hinrichs J. Flapless alveolar ridge preservation utilizing the "socket-plug" technique: clinical technique and review of the literature. *J Oral Implantol.* 2014;40:690-8.
26. Di Carlo S, De Angelis F, Brauner E, Rosella D, Papi P, Pompa G, et al. Histological and immunohistochemical evaluation of mandibular bone tissue regeneration. *Int J Immunopathol Pharmacol.* 2018;32:2058738418798249.
27. Nanes BA. Slide Set: Reproducible image analysis and batch processing with ImageJ. *Biotechniques.* 2015;59:269-78.
28. Shin M, Izumi S, Nakane PK. Multilayer peroxidase-labeled antibody method: comparison with labeled streptavidin-biotin method, avidin-biotin-peroxidase complex method, and peroxidase-antiperoxidase method. *J Clin Lab Anal.* 1995;9:424-30.
29. Farina R, Trombelli L. Wound healing of extraction sockets. *Endodon Top.* 2011;25:16-43.
30. Aukhil I. Biology of wound healing. *Periodontol 2000.* 2000;22:44-50.
31. Laureti M, Ferrigno N, Rosella D, Papi P, Mencio F, De Angelis F, et al. Unusual Case of Osseointegrated Dental Implant Migration into Maxillary Sinus Removed 12 Years after Insertion. *Case Rep Dent.* 2017;2017:9634672.
32. Sakamoto, M. Development and evaluation of superporous hydroxyapatite ceramics with triple pore structure as bone tissue scaffold. *J Ceram Soc JAPAN.* 2010;118:753-7.
33. Ojala T, Lehtinen R. The importance of alveolar bone loss, width of periodontal space, visibility of lamina dura and divergence of roots on the rocking moments in extraction of teeth in the lower jaw. *Int J Oral Surg.* 1980;9:373-6.
34. Woodard JR, Hilldore AJ, Lan SK, Park CJ, Morgan AW, Eurell JA, et al. The mechanical properties and osteoconductivity of hydroxyapatite bone scaffolds with multi-scale porosity. *Biomaterials.* 2007;28:45-54.
35. Hua Y, Ning C, Xiaoying L, Buzhong Z, Wei C, Xiaoling S. Natural hydroxyapatite/chitosan composite for bone substitute materials. *Conf Proc IEEE Eng Med Biol Soc.* 2005;2005:4888-91.
36. Zhao R, Xie P, Zhang K, Tang Z, Chen X, Zhu X, et al. Selective effect of hydroxyapatite nanoparticles on osteoporotic and healthy bone formation correlates with intracellular calcium homeostasis regulation. *Acta Biomater.* 2017;59:338-50.
37. Kong L, Gao Y, Lu G, Gong Y, Zhao N, Zhang X. A study on the bioactivity of chitosan/nano-hydroxyapatite composite scaffolds for bone tissue engineering. *Eur Polym J.* 2006;42:3171-9.
38. Liu H, Peng H, Wu Y, Zhang C, Cai Y, Xu G, et al. The promotion of bone regeneration by nanofibrous hydroxyapatite/chitosan scaffolds by effects on integrin-BMP/Smad signaling pathway in BMSCs. *Biomaterials.* 2013;34:4404-17.
39. Lai CF, Cheng SL. Alphavbeta integrins play an essential role in BMP-2 induction of osteoblast differentiation. *J Bone Miner Res.* 2005;20:330-40.
40. da Silva de Oliveira JC, Luvizuto ER, Sonoda CK, Okamoto R, Garcia-Junior IR. Immunohistochemistry evaluation of BMP-2 with β -tricalcium phosphate matrix, polylactic and polyglycolic acid gel, and calcium phosphate cement in rats. *Oral Maxillofac Surg.* 2017;21:247-58.
41. Denhardt DT, Guo X. Osteopontin: a protein with diverse functions. *FASEB J.* 1993;7:1475-82.
42. Rajee MM, Ashma R. Epigenetic regulation of BMP2 gene in osteoporosis: a DNA methylation study. *Mol Biol Rep.* 2019;46:1667-74.